GOLDSCHMIDT, G. H. & LLEWELLYN, F. J. (1950). *Acta Cryst.* **3**, 294.
HOWELLS, E. R., PHILLIPS, D. C. & ROGERS, D. (1950). *Acta Cryst.* **3**, 210.
HUNTER, L. (1945). *J. Chem. Soc.* p. 506.
LIPSON, H. & WOOLFSON, M. M. (1952). *Acta Cryst.* **5**, 680.
OVEREND, W. G. (1946). Ph.D. Thesis, University of Birmingham.
RENNINGER, M. Z. (1937). *Z. Kristallogr.* **97**, 107.
VAUGHAN, P. & DONOHUE, J. (1952). *Acta Cryst.* **5**, 530
WIGGINS, L. F., GREGORY, H., OVEREND, W. G. & HOMER, R. F. (1948). *J. Chem. Soc.* p. 2197.
WILSON, A. J. C. (1951). *Research, Lond.* **4**, 141.

Acta Cryst. (1954). **7**, 203

X-ray Study of Phase Transitions in $PbZrO_3$ Containing Ba or Sr*

BY GEN SHIRANE† AND SADAO HOSHINO
Tokyo Institute of Technology, Oh-okayama, Tokyo, Japan

(*Received* 6 *February* 1953 *and in revised form* 23 *June* 1953)

The crystal structures of various phases in (Pb–Ba)ZrO_3 and (Pb–Sr)ZrO_3 systems, the dielectric properties of which were reported previously, have been studied by the powder diffraction method. A crystal structure of a ferroelectric intermediate phase in the (Pb–Ba)ZrO_3 system, which can be observed between the antiferroelectric (tetragonal) and paraelectric (cubic) phases found in pure $PbZrO_3$ when the Ba concentration exceeds 5%, is shown to be a rhombohedral modification of the perovskite structure with α slightly less than 90°. It is shown that, although the (Pb–Ba)ZrO_3 compositions from pure $PbZrO_3$ to (Pb95–Ba5)ZrO_3 do not show this intermediate phase, the application of a strong d.c. field can produce the rhombohedral phase just below their Curie temperatures. A crystal structure of an intermediate antiferroelectric phase in the (Pb–Sr)ZrO_3 system, which begins to appear when the concentration of Sr is as small as 1%, is found to have a tetragonal lattice with c/a slightly less than unity. The observed superlattice lines in this phase are different from those of the antiferroelectric phase in pure $PbZrO_3$.

1. Introduction

A previous investigation (Shirane, 1952) of the dielectric, dilatometric, and calorimetric properties of $PbZrO_3$ containing Ba or Sr has shown the existence of a new intermediate phase besides the antiferroelectric and paraelectric phases found in pure $PbZrO_3$ (Sawaguchi, Shirane & Takagi, 1951). The phase diagrams of the (Pb–Ba)ZrO_3 and (Pb–Sr)ZrO_3 systems determined by the dielectric measurements are shown in Fig. 1. In the (Pb–Ba)ZrO_3 system, the dielectric properties of the intermediate phase are certainly of the ferroelectric type. In the (Pb–Sr)ZrO_3 system, on the other hand, the dielectric response of the intermediate phase can be well explained if we assume this phase to be antiferroelectric, not ferroelectric.

According to Megaw (1946), the crystal structure of $PbZrO_3$ at room temperature is a tetragonal modification of the perovskite structure with $a = 4{\cdot}150$ kX. and $c/a = 0{\cdot}988$. This crystal structure differs from that of ferroelectric $BaTiO_3$ (Megaw, 1946, 1947) in two important respects: first, the axial ratio is less than unity in contrast with the value of 1·01 in $BaTiO_3$, and secondly, some extra lines in addition to the ordinary tetragonal multiplets can be observed. The X-ray analysis of single crystals by Sawaguchi,

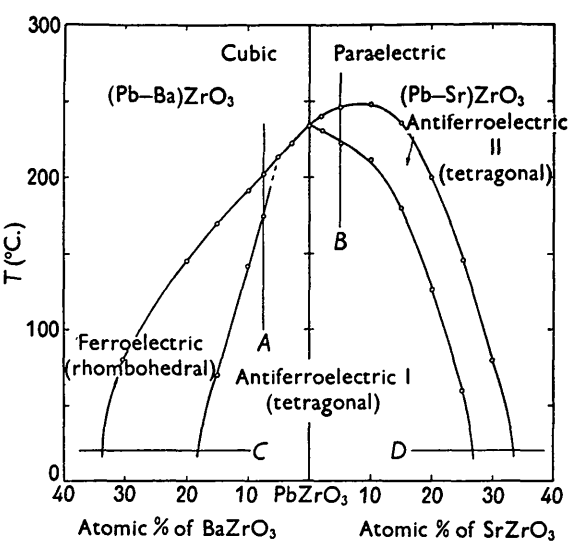

Fig. 1. Phase diagrams of (Pb–Ba)ZrO_3 and (Pb–Sr)ZrO_3 (after Shirane).

* The expense of this research was defrayed from the Scientific Research Expenditure of the Japanese Ministry of Education.

† Now at Department of Physics, Pennsylvania State College, State College, Pennsylvania, U.S.A.

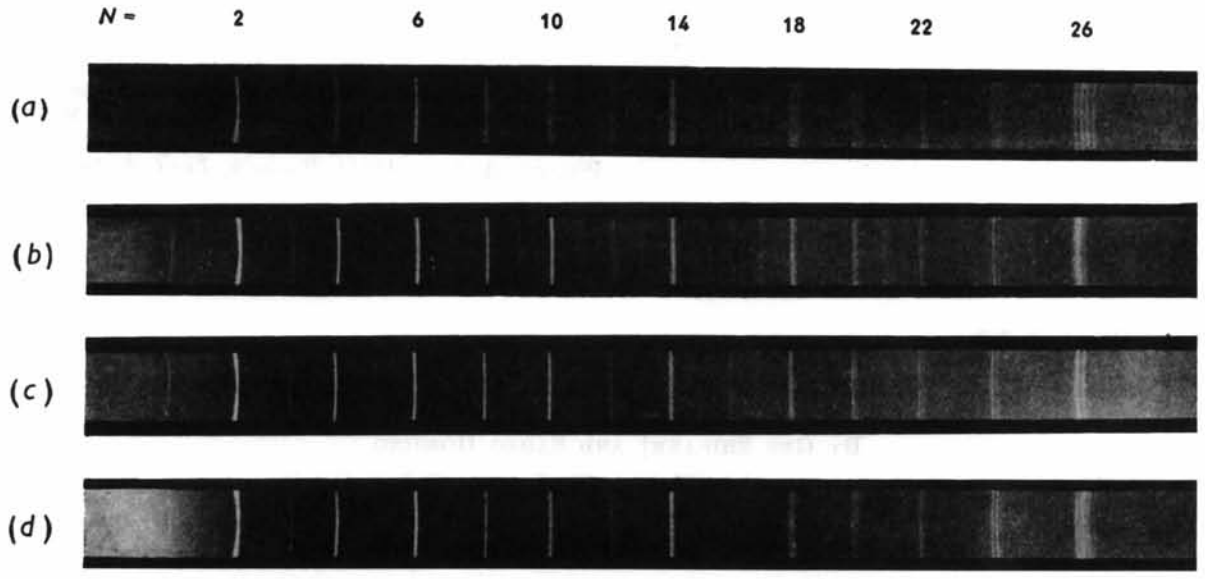

Fig. 2. Powder photographs taken with Cu $K\alpha$ radiation. (*a*)–(*c*) (Pb92·5–Ba7·5)ZrO_3: (*a*) 150° C.—tetragonal, $c/a = 0{\cdot}993$; (*b*) 185° C.—rhombohedral, $\alpha = 89° 52'$; (*c*) 210° C.—cubic. (*d*) (Pb95–Sr5)ZrO_3: 230° C.—tetragonal, $c/a = 0{\cdot}9955$.

Maniwa & Hoshino (1951) has revealed that these extra lines should be attributed to a superlattice due to the antiparallel displacement of Pb ions in the [110] and [$\bar{1}$10] directions. Therefore, their true symmetry is probably orthorhombic. However, powder diffraction patterns as well as single-crystal oscillation photographs have shown that the orthorhombic distortion from a tetragonal lattice is negligibly small.

An X-ray study of the phase transition in $PbZrO_3$ at about 230° C. was carried out by Ueda & Shirane (1951) by the powder diffraction method. It was shown that there exists a large volume expansion at the transition point and that the extra lines observed in the antiferroelectric phase disappear completely in the cubic region above the Curie point. Recently, a more detailed X-ray study of the variation of the lattice parameters near the Curie point was made by Sawaguchi (1952) on a high-purity ceramic specimen.

Our primary concern in this paper is to study the crystal structures, and their relation to the dielectric properties, of the various phases, and especially the intermediate phases, in the (Pb–Ba)ZrO_3 and (Pb–Sr)ZrO_3 systems by comparing the results with those of pure $PbZrO_3$. For this purpose the structure changes with temperature for two compositions (Pb92·5–Ba7·5)ZrO_3 and (Pb95–Sr5)ZrO_3 were studied by the X-ray powder method (sections *A* and *B* in Fig. 1). Then the structure of the whole concentration range of these two solid-solution systems was studied at room temperature (sections *C* and *D* in the same figure).

All of the specimens of (Pb–Ba)ZrO_3 and (Pb–Sr)ZrO_3 compositions used in the present experiments are the same as those used in the previous dielectric study (Shirane, 1952). They were made from the appropriate mixture of PbO, ZrO_2 and $BaCo_3$ or $SrCO_3$ by sintering at temperatures between 1200 and 1350° C.

2. Phase transition in (Pb92·5–Ba7·5)ZrO_3

The structure changes which take place at the two phase boundaries in (Pb–Ba)ZrO_3 compositions were studied for the specimen of (Pb92·5–Ba7·5)ZrO_3. As shown by the foregoing investigations, this solid solution transforms, at rising temperature, from the antiferroelectric phase to the ferroelectric one at 175° C. and further to the paraelectric phase at the Curie point of 200° C. (Fig. 1). The sintered disc was pulverized to a fine powder and formed with starch into a rod about 0·3 mm. in diameter. A 55·5 mm. radius high-temperature X-ray camera was used with a furnace surrounding the specimen, which can be kept at a constant temperature within ±1° C. during the exposure. The X-ray photographs were taken with Cu $K\alpha$ radiation and a Ni foil filter 0·01 mm. thick. In the photographs of this specimen, the Cu $K\alpha$ doublet could be resolved at $\theta = 40°$.

The Debye–Scherrer photographs taken at 150, 185 and 210° C. are shown in Fig. 2. The diffraction patterns at 150° C., which correspond to the antiferroelectric phase, can be explained by assuming a tetragonal structure with $a = 4{\cdot}152$ kX. and $c/a = 0{\cdot}993$.* This is the same lattice type as that of pure $PbZrO_3$. Moreover, the extra lines observed in this photograph are all of the same nature as those found in pure $PbZrO_3$ with respect to the relative intensities as well as to the spacing. The structure of the paraelectric

* $\lambda = 1{\cdot}5374$ kX. was used as the value of the Cu $K\alpha_1$ wavelength for the convenience of comparison with previous data.

phase above the Curie point of 200° C. has a cubic lattice without any superlattice.

The high-order reflections in the photograph taken at 185° C., which is in the ferroelectric phase, show slight but definite line splittings, the photometry curves of which are shown in Fig. 3. These line splittings can be explained if we assume a rhombohedral lattice with α slightly less than 90°. This possibility is strongly supported by the fact that the (400) group shows no multiplet structure except the doublet due to $K\alpha_1$ and $K\alpha_2$. On assuming this lattice type, calculations of α can be made independently for each of the four line groups in Fig. 3, in which the line indices assumed for the calculation are shown.* The angles calculated from each of the four line groups agreed well with each other giving $\alpha = 89° 52' \pm 1'$. Assuming this value of α, the axial parameter a was calculated from the (510), (431) line group as $a = 4{\cdot}153(\pm 0{\cdot}001)$ kX.

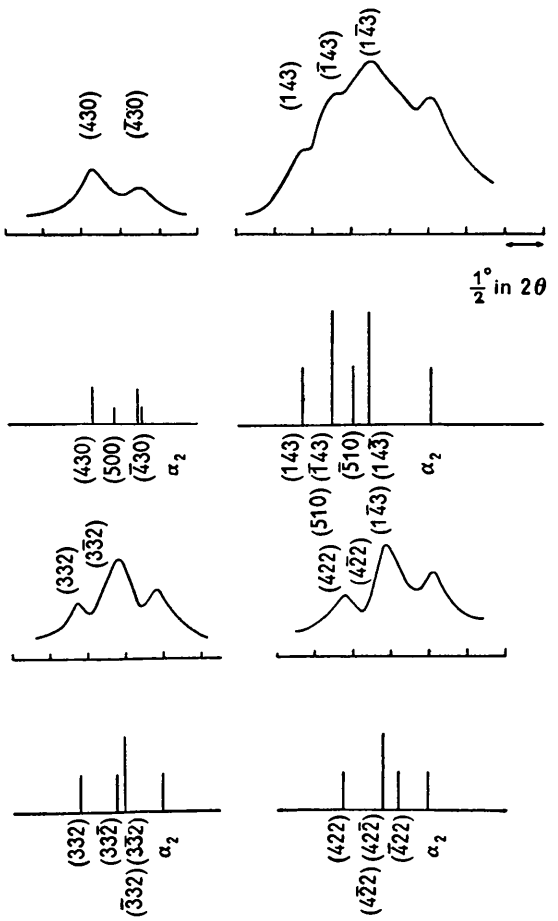

Fig. 3. Photometry curves of high-order line groups with $N = 22$, 24, 25, and 26 of $(Pb92{\cdot}5–Ba7{\cdot}5)ZrO_3$ at 185° C. The calculated intensity relation of a rhombohedral lattice with $a = 4{\cdot}153$ kX. and $\alpha = 89° 52'$ are shown below for comparison.

All the lattice spacings for high-order multiplets have been calculated by assuming the above lattice constants. Some of the results are shown in Fig. 3, where they are compared with the observed line splittings. For simplicity, the lines due to $K\alpha_2$ radiation are omitted except for the important ones. Though some weak lines, such as $(\bar{5}10)$, (500), $(\bar{4}22)$ and $(33\bar{2})$, are not well resolved in the observed curves, the agreement is satisfactory for the main lines not only in their spacings but also in the relative intensities. Thus the conclusion is that the crystal structure of the intermediate phase in $(Pb92{\cdot}5–Ba7{\cdot}5)ZrO_3$ has a rhombohedral lattice with $\alpha < 90°$. This structure has the same symmetry as observed in $BaTiO_3$ below −70° C. (Kay & Vousden, 1949), and, since the lattice distortion from the ideal cubic cell is produced by a slight extension along a triad axis, the polar axis is in the [111] direction.

It should be added here that a careful comparison of powder photographs of the three phases (Fig. 2) has revealed striking intensity anomalies in the ferroelectric phase. It is seen that in the intermediate phase the lines with odd $N = h^2+k^2+l^2$ show anomalously strong intensity in comparison with even N lines, even at low orders, while the corresponding lines in the lowest tetragonal phase have similar intensity to that in the cubic phase.

This intensity anomaly becomes more prominent in the high-order lines. In addition, the intensity relation of the multiplet lines in a group with odd N does not agree with the calculated one which was obtained by assuming a cubic perovskite structure with the atoms at the special positions in the unit cell. The common characteristic of the discrepancy is that in a certain multiplet the line with largest value of $|h+k+l|$ always shows a stronger intensity than expected from the calculation. For example, the (430) $(\bar{4}30)$ line is about two times stronger than the $(\bar{4}30)$ $(4\bar{3}0)$ line, whereas they should have the same intensity according to the calculation. This (430) group is, unfortunately, the only one with odd N among the well resolved groups, but a similar tendency can be observed in other high-order groups.

These intensity anomalies can be explained qualitatively if we assume a suitable ion shift in a rhombohedral lattice. The structure factor for an ideal cubic cell of the perovskite-type structure is

$$\left.\begin{aligned} F_1 &= f_{Pb}-f_O-f_{Zr} \quad \text{(one of } h, k \text{ or } l \text{ is odd)} \\ F_2 &= f_{Pb}+3f_O-f_{Zr} \quad \text{(all of } h, k \text{ and } l \text{ are odd)} \end{aligned}\right\} \text{odd } N$$

$$\left.\begin{aligned} F_3 &= f_{Pb}-f_O+f_{Zr} \quad \text{(one of } h, k \text{ or } l \text{ is even)} \\ F_4 &= f_{Pb}+3f_O+f_{Zr} \quad \text{(three of } h, k \text{ and } l \text{ are even)} \end{aligned}\right\} \text{even } N$$

when the atomic positions are (0, 0, 0) for Pb, $(\frac{1}{2}, \frac{1}{2}, \frac{1}{2})$ for Zr and $(\frac{1}{2}, \frac{1}{2}, 0)$, $(\frac{1}{2}, 0, \frac{1}{2})$ and $(0, \frac{1}{2}, \frac{1}{2})$ for 3 O.

* Since the $(\bar{4}22)$ and $(33\bar{2})$ lines are not well resolved (see Fig. 3), we indexed the stronger lines in the groups as $(4\bar{2}2)$ $(42\bar{2})$ and $(\bar{3}32)$ $(3\bar{3}2)$ for the calculation of α from (422) and (332) groups. The ambiguity introduced by this approximation is $\pm 1'$. The same method is used throughout this paper whenever we calculate α from these line groups.

In the rhombohedral structure, the ferroelectricity may be due to the parallel displacement of Zr or Pb ions along a [111] direction and the associated displacements of three oxygen ions. The displacements of oxygen ions were neglected for simplicity and it was assumed that Zr ions were being displaced to $(\frac{1}{2}+\delta, \frac{1}{2}+\delta, \frac{1}{2}+\delta)$. As a result of this displacement the square of the structure factor F^2 for each reflection changes to

$$\left.\begin{aligned} &F_1^2+2(f_{Pb}-f_O)f_{Zr}(1-\cos 2\pi\delta(h+k+l)) \\ &F_2^2+2(f_{Pb}+3f_O)f_{Zr}(1-\cos 2\pi\delta(h+k+l)) \end{aligned}\right\} \text{for odd } N$$

$$\left.\begin{aligned} &F_3^2-2(f_{Pb}-f_O)f_{Zr}(1-\cos 2\pi\delta(h+k+l)) \\ &F_4^2-2(f_{Pb}+3f_O)f_{Zr}(1-\cos 2\pi\delta(h+k+l)) \end{aligned}\right\} \text{for even } N$$

These equations show: (1) the line intensity for odd N increases in relation to that of even N; (2) in the given group of odd N, the anomaly is an increasing function of $|h+k+l|$. Thus the observed intensity anomalies are explained qualitatively. These equations show that some anomaly should also be found in a given group with even N, but this anomaly seems to be covered by the strong intensity of these groups. By assuming that Pb ions are being displaced, similar results can be obtained.

The temperature change of the lattice parameters was calculated from the (510) line group and is shown in Fig. 4. At the transition region around 175° C.,

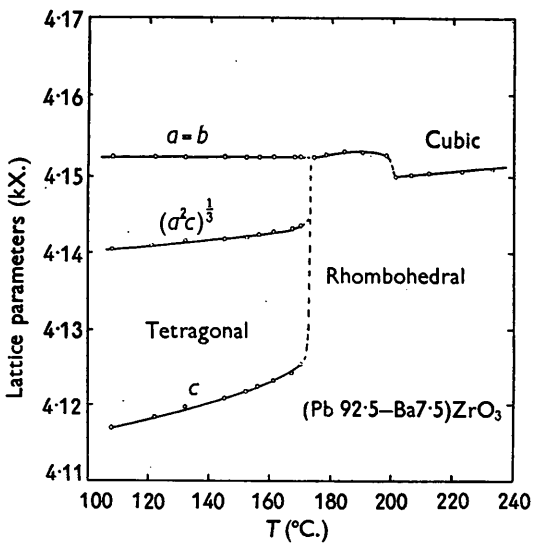

Fig. 4. Lattice spacing *v.* rising temperature curve of $(Pb92{\cdot}5\text{–}Ba7{\cdot}5)ZrO_3$.

c increases considerably until it coincides with a, which is almost constant through the transition. At the same time, the structure changes to a rhombohedral lattice with $\alpha = 89°\ 52'$. It should be noted here that the increase in unit-cell volume at this transition is very large, being 0·48 kX.^{3}. In the ferroelectric phase between 175 and 200° C., the angle of distortion, α, is nearly constant. At the Curie point of 200° C., the structure changes suddenly to an ideal cubic one accompanied by a decrease of the unit cell volume of 0·15 kX.^{3}. The superlattice lines observed at room temperature remain almost constant in their spacings at temperatures below 175° C., but their intensities decrease gradually. Above 175° C., no extra lines can be observed in either the ferroelectric or paraelectric regions.

3. Crystal structure of (Pb–Ba)ZrO_3

The crystal structure in the whole concentration range of (Pb–Ba)ZrO_3 compositions at room temperature was studied by using a powder camera (35 mm. radius) and Cu $K\alpha$ radiation (Fig. 5). The compositions from

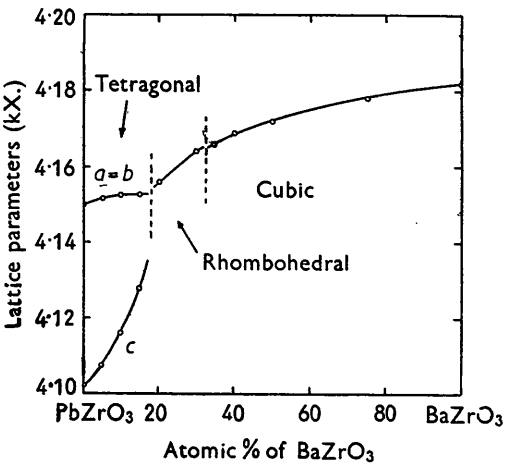

Fig. 5. Lattice parameters *v.* composition curve for (Pb–Ba)ZrO_3.

pure $PbZrO_3$ to $(Pb85\text{–}Ba15)ZrO_3$, which are antiferroelectric at room temperature, give Debye–Scherrer diffraction patterns showing multiplets which are obviously due to a tetragonal structure with $c/a < 1$. The axial ratio approaches unity when the Ba concentration increases, reaching 0·994 at $(Pb85\text{–}Ba15)ZrO_3$ and it shows a sudden jump at a certain composition between $(Pb85\text{–}Ba15)ZrO_3$ and $(Pb80\text{–}Ba20)ZrO_3$, at which the dielectric properties change from antiferroelectric to ferroelectric.

The characteristics of the powder photographs of the $(Pb80\text{–}Ba20)ZrO_3$ and $(Pb70\text{–}Ba30)ZrO_3$ compositions are of the same nature as observed in the ferroelectric phase in $(Pb92{\cdot}5\text{–}Ba7{\cdot}5)ZrO_3$. Sufficient resolution is not obtained for the (510) (431) line group because of the line broadening which may be attributed to strain inhomogeneity inevitably associated with solid solutions; yet the (422) and (332) line groups show the same line splitting which indicates a small rhombohedral distortion from the cubic lattice. The angle of distortion, α, is $89°\ 52' \pm 1'$. Anomalous intensities of odd-N groups are also observed in this case. When the electric properties change from ferroelectric to paraelectric at the $(Pb65\text{–}Ba35)ZrO_3$ composition, the structure changes to an ideal cubic one. The lattice

constant of pure $BaZrO_3$ is in satisfactory agreement with the data of Megaw (1946).

The superlattice lines observed in pure $PbZrO_3$ are also observed in the photographs of the antiferroelectric tetragonal range, with a slight decrease in intensities with increasing Ba concentration. No extra lines can be observed in either the ferroelectric or the paraelectric state.

4. Forced transition by electric field

Fig. 1 shows that the ferroelectric intermediate phase in (Pb–Ba)ZrO_3 compositions does not appear until the Ba concentration exceeds the threshold value of about 5%. In the compositions from pure $PbZrO_3$ to (Pb95–Ba5)ZrO_3, however, the application of a strong electric field is able to change the antiferroelectric state to the ferroelectric one at temperatures just below the Curie point. As was shown by the detailed study (Shirane, 1952) of (Pb97–Ba3)ZrO_3, this 'forced transition' can be realized by an a.c. as well as a d.c. electric field. This forced ferroelectric phase seems likely to be the same as the intermediate phase observed in (Pb92·5–Ba7·5)ZrO_3, the structure of which, as mentioned before, has now turned out to be based on a rhombohedral lattice. Another possibility is that by a strong electric field the antiparallel dipole arrangement in the [110] direction is forced to change to the parallel one. In the latter case the original pseudo-tetragonal structure will be kept unchanged. To decide between these alternatives, an X-ray study has been carried out with the specimen under a d.c. field of sufficient strength to cause the forced transition.

The difficulty in the study of this forced transition lies in the fact that the realization of this transition is limited to a narrow temperature range just below the Curie point; for example, (Pb97–Ba3)ZrO_3 becomes ferroelectric only between 216 and 222° C. under the d.c. field of 15 kV.cm.$^{-1}$. At such temperatures, the Debye–Scherrer photographs usually show diffuse lines due to the large strain inhomogeneity associated with the phase transition even without d.c. field. To get a sufficiently large temperature range, the specimen of (Pb95–Ba5)ZrO_3 was used on which the ferroelectric phase can be realized by the same d.c. field of 15 kV.cm.$^{-1}$ between 196 and 215° C., as shown in the permittivity curves in Fig. 6.

The experimental arrangement is, in principle, similar to that used by Danielson (1949) for the study of domain orientation of polycrystalline $BaTiO_3$. The samples were in the form of ceramic plates 2×4 mm.^{2} in area and 0·5 mm. in thickness with silver electrodes evaporated on both surfaces. These plates were mounted at the center of the same high-temperature camera as was formerly used for the study of (Pb92·5–Ba7·5)ZrO_3. The incident X-ray beam (Cu $K\alpha$) was nearly perpendicular to the electrode surface of the specimen.

Photographs were taken at 202° C. with a stationary specimen. When no electric field is applied, diffraction patterns show the multiplets due to a tetragonal lattice with $a = 4{\cdot}152$ kX. and $c/a = 0{\cdot}9935$. Application of

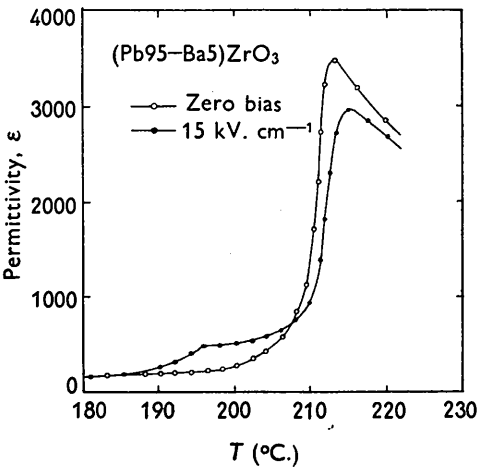

Fig. 6. Permittivity v. rising temperature curves of (Pb95–Ba5)ZrO_3. 1 Mc./sec.

the d.c. field of 15 kV.cm.$^{-1}$ changes these patterns so that they become very similar to those of the rhombohedral phase in (Pb92·5–Ba7·5)ZrO_3, especially in the following two important points. First, the (422) and (332) line groups show multiplets of essentially the same nature as shown in Fig. 3 (see Fig. 7).

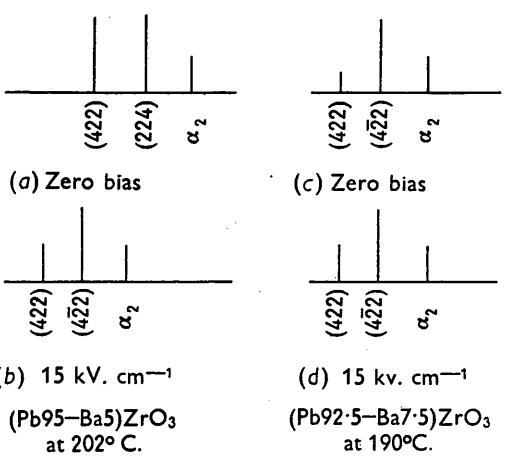

Fig. 7. The change in the line characteristic of the (422) group by the application of a d.c. field of 15 kV. cm.$^{-1}$.

Secondly, the intensity of the groups with odd N, such as (430), (421) and (331), increases remarkably compared with those of the tetragonal phase. From these facts we can conclude that the forced ferroelectric phase has also a rhombohedral lattice with $\alpha < 90°$. The lattice parameters calculated from the (430), (422) and (332) groups are $a = b = c = 4{\cdot}153$ kX. and $\alpha = 89°\ 53'$. Attention should be paid to the

fact that the unit-cell volume increases remarkably during the forced transition, namely from 71·11 kX.[3] in the tetragonal phase to 71·63 kX.[3] in the rhombohedral one. This difference, 0·52 kX.[3], is of the same order of magnitude as the volume change at the tetragonal *v.* rhombohedral transition in (Pb92·5–Ba7·5)ZrO_3.

The above experiments have made clear the fact that the crystal structure of the forced ferroelectric phase in (Pb95–Ba5)ZrO_3 is essentially similar to that of the intermediate phase in (Pb92·5–Ba7·5)ZrO_3. Careful comparison of the diffraction patterns of these two phases, however, has revealed an interesting intensity relation. In the forced phase, an increase in the relative intensities of (422) to ($4\bar{2}2$), (332) to ($3\bar{3}2$) and (420) to ($\bar{4}20$) is noticed. This intensity anomaly can be explained easily if it is assumed that in this phase the remarkable domain alignment does occur in such a way that the [111] direction of each domain becomes as parallel to the electric field as possible. This orientation results in an increase of the (422), ($\bar{3}32$) and (420) intensities over those expected for the case of random distribution. To confirm whether this anomaly is actually due to domain orientation or not, a powder photograph was taken of (Pb92·5–Ba7·5)ZrO_3 at 190° C. under the application of the d.c. field of 15 kV.cm.$^{-1}$, and it was found that the intensity relation was changed considerably by the d.c. field. It was confirmed that the line characteristics for this specimen under a d.c. field are exactly of the same nature as observed in the forced ferroelectric phase in (Pb95–Ba5)ZrO_3. Fig. 7 shows schematically the intensity variation in the (422) line group caused by the application of a d.c. field.

Previously, in the course of the dielectric study of pure $PbZrO_3$ (Shirane, Sawaguchi & Takagi, 1951) we found that the specimen is sometimes reduced to powder state by the repeated applications of a strong a.c. field which causes the forced transition. Now this phenomenon can be understood if we take into account the fact that the forced transition is accompanied by a large volume change of about 0·5 kX.[3], as shown by the above experiments. Repetition of such a large volume change seems to cause internal cracks, sometimes sufficient for the disintegration of the sample.

5. Phase transition in (Pb95–Sr5)ZrO_3

The structure changes at the two phase boundaries in (Pb–Sr)ZrO_3 compositions were studied for the specimen of (Pb95–Sr5)ZrO_3. The dielectric and thermal investigations have shown that (Pb95–Sr5)ZrO_3 transforms at rising temperature from an antiferroelectric phase to another antiferroelectric phase at 222° C. and further to a paraelectric phase at 245° C. These two phase transitions have been studied with powder photographs by using the same high-temperature camera as was used for the study of (Pb92·5–Ba7·5)ZrO_3.

Below 222° C., the crystal structure is similar to that of pure $PbZrO_3$ and the lowest phase of (Pb92·5–Ba7·5)ZrO_3, i.e. a tetragonal lattice with $c/a = 0·99$ and with the same superlattice. Above 245° C. the structure has a cubic lattice without any superlattice.

The characteristics of the line splittings in the photograph at 230° C. (Fig. 2(*d*)) show its symmetry to be probably tetragonal with the axial ratio very close to unity. Assuming a tetragonal structure, the lattice constant a and axial ratio c/a are calculated from the (422) and (510) (134) groups independently. The results are in good agreement with each other and give the values $a = 4·147(\pm 0·001)$ kX. and $c/a = 0·9955(\pm 0·0005)$. We have calculated the distribution of all multiplets of these two groups by using the above parameters and have compared them with the observed photometry curves (Fig. 8). The agreement is

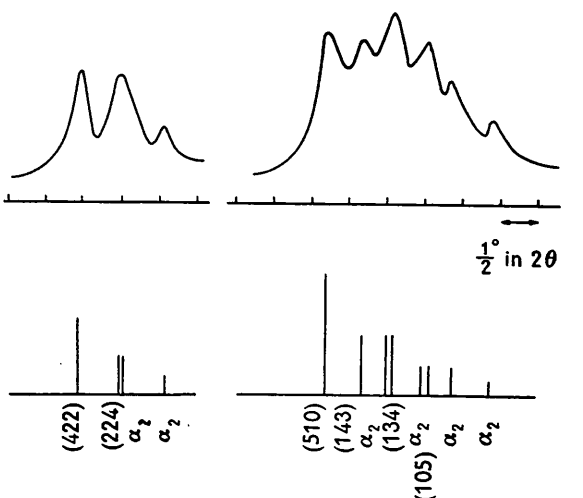

Fig. 8. Photometry curves of (422) and (510) (134) line groups of (Pb95–Sr5)ZrO_3 at 230° C. and the calculated intensity relation of a tetragonal lattice with $a = 4·147$ kX. and $c/a = 0·9955$.

satisfactory in the spacings as well as in relative intensities within each group. All other lines can be well explained with these axial parameters. It should be added that the anomalous intensity relations observed in the intermediate phase in (Pb92·5–Ba7·5)ZrO_3 are not detected here.

The dielectric study of this composition has shown that the intermediate phase is antiferroelectric and not ferroelectric. If this is the case, some superlattice lines should be observed in this phase because their existence is the necessary condition for antiferroelectricity. In fact, some extra lines are found though they are rather faint. A careful comparison of these extra lines with those of the lowest phase has revealed that both are different not only in the spacing but also in relative intensities. They show that the antiferroelectricity of the intermediate phase is due to a different type of ion displacement from that in the lowest phase.

Although it may be difficult to obtain detailed information about the ion displacement from the sole

Table 1. *Anomalous volume contraction or expansion ($\Delta v/v$) estimated from the extrapolation of the linear part in the cubic phase*

Composition	Lowest phase	Intermediate phase
$PbZrO_3$	-41×10^{-4} at 230° C.	—
$(Pb92{\cdot}5–Ba7{\cdot}5)ZrO_3$	-43×10^{-4} at 150° C.	$+24\times10^{-4}$ at 190° C.
$(Pb95–Sr5)ZrO_3$	-30×10^{-4} at 210° C.	-20×10^{-4} at 230° C.

knowledge of the superlattice lines in a powder photograph, the following consideration may be helpful. It was found that some of the observed superlattice lines cannot be indexed unless we use smaller fractions than $\frac{1}{4}$ of $(h^2+k^2+l^2)$. This indicates that one or more spacings of the superlattice must have a longer period than twice the single cell edge .and, therefore, the possibility of a simple model for antiferroelectricity, such as a tetragonal lattice with the alternating polarized line arrangement of dipoles (Luttinger & Tisza, 1946; Kittel, 1951) is ruled out. To make clear the true origin of the antiferroelectricity we must wait for optical and structural studies of single crystals of the same composition.

The temperature change of lattice parameters calculated from the (510) and (134) lines is shown in Fig. 9. Around the transition at 222° C., the a axis

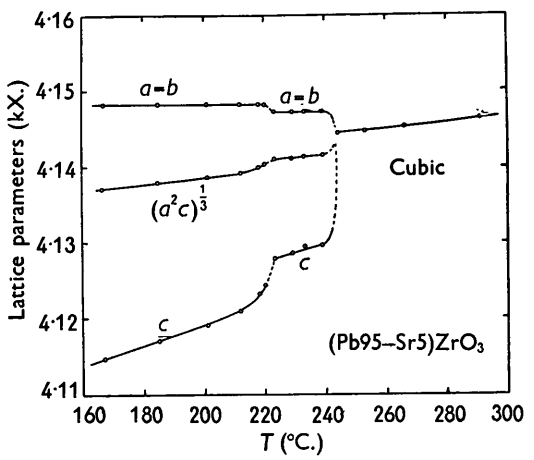

Fig. 9. Lattice spacing v. rising temperature curve of $(Pb95–Sr5)ZrO_3$.

suddenly shows a small decrease while the c axis increases, resulting in a jump of the axial ratio c/a. The unit-cell volume shows a gradual increase in the neighborhood of this transition point and a sharp increase of 0·16 kX.[3] at the upper transition point, 245° C.

It is interesting to compare these volume changes with the results observed at the corresponding two phase transitions in $(Pb92{\cdot}5–Ba7{\cdot}5)ZrO_3$ (Fig. 4). To show these peculiar volume changes from another viewpoint, we have compared the actual volume with the extrapolated volume from the cubic phase and estimated the anomalous volume expansion or contraction associated with the ferroelectric or antiferroelectric dipole arrangement. The results are shown in Table 1 together with those of pure $PbZrO_3$ (Sawaguchi, 1952). Estimated volume expansion coefficients in the lowest phase and in the cubic phase for these three compounds are shown in Table 2. These results

Table 2. *Volume expansion coefficient*

Composition	Lowest phase	Cubic phase
$PbZrO_3$	27×10^{-6}/°C.	33×10^{-6}/°C.
$(Pb92{\cdot}5–Ba7{\cdot}5)ZrO_3$	22	23
$(Pb95–Sr5)ZrO_3$	24	32

are in qualitative agreement with the previous dilatometric data (Shirane, 1952).

6. Crystal structure of $(Pb–Sr)ZrO_3$

The lattice spacing v. composition curve of the $(Pb–Sr)ZrO_3$ system was obtained from the (510) line group (Fig. 10). In the lowest antiferroelectric phase

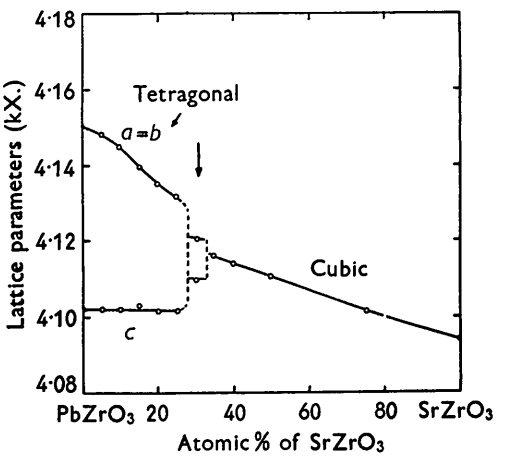

Fig. 10. Lattice parameters v. composition curve for $(Pb–Sr)ZrO_3$.

from pure $PbZrO_3$ to $(Pb75–Sr25)ZrO_3$ compositions, the diffraction patterns are all of the same nature as those of pure $PbZrO_3$, not only in the multiplets due to a tetragonal lattice with $c/a < 1$, but also in the behavior of the superlattice lines. The axial ratio c/a gradually approaches unity with increasing Sr concentration, accompanied by a decrease in the intensity of the superlattice lines. In the paraelectric region from $(Pb65–Sr35)ZrO_3$ up to pure $SrZrO_3$, the structure has a cubic lattice without any superlattice.

The diffraction patterns of $(Pb70–Sr30)ZrO_3$, which is in the intermediate phase at room temperature,

cannot be well resolved because of line broadening which may be attributed to the large strain inhomogeneity. Close inspection of high-order lines, however, showed that the structure may have a tetragonal lattice with c/a only slightly less than unity. Assuming this structure, c/a is calculated as $0{\cdot}997\pm0{\cdot}001$. We found some extra lines, but they are too faint to ascertain whether or not they are similar to those observed in (Pb95–Sr5)ZrO_3 at 230° C. To study this point from another side, powder photographs of (Pb98–Sr2)ZrO_3, (Pb90–Sr10)ZrO_3, and (Pb80–Sr20)ZrO_3 were taken at temperatures corresponding to the intermediate phase of each compound. Comparison of these photographs with that of (Pb70–Sr30)ZrO_3 shows that all of them have the same type of pattern, with gradual change of axial ratio c/a and gradual increase in line broadening with increasing Sr concentration. It seems, therefore, that the whole range of the intermediate phase in the (Pb–Sr)ZrO_3 system probably has a similar structure to that found in (Pb95–Sr5)ZrO_3.

7. Concluding remarks

It is known (Shirane & Takeda, 1952) that when some of the Zr ions in $PbZrO_3$ are replaced by Ti ions, a ferroelectric phase appears between the antiferroelectric and paraelectric phases of pure $PbZrO_3$. The close resemblances of the dielectric and dilatometric properties of this ferroelectric phase with those of the corresponding phase in the (Pb–Ba)ZrO_3 system suggested that they both may be similar, though crucial evidence had not been obtained. Very recent reexamination (Shirane & Hoshino, 1952) of the structure of the ferroelectric phase in Pb(Zr95–Ti5)O_3 has shown that this phase has also a rhombohedral lattice with $\alpha < 90°$ as in the present case of (Pb92·5–Ba7·5)ZrO_3.

Thus the ferroelectric Curie point in $PbZrO_3$ containing Ba or Ti has been shown to correspond to a transition from cubic to rhombohedral. This conclusion is unexpected because all of the other perovskite-type ferroelectrics such as $BaTiO_3$, $KNbO_3$ (Wood, 1951), etc. transform, at falling temperature, in the well accepted sequence: cubic–tetragonal–orthorhombic–rhombohedral. The explanation of this difference from the atomic viewpoint is an interesting problem in ferroelectricity, especially in connection with the fact that, as reported formerly, the free energy of this rhombohedral phase is very close to that of the two antiferroelectric phases near the Curie point of pure $PbZrO_3$.

We wish to express our sincere thanks to Prof. Y. Takagi and S. Miyake for their very illuminating suggestions, and to Messrs E. Sawaguchi and K. Suzuki for their helpful discussions during the course of this work. Thanks are also due to Prof. R. Pepinsky and T. Watanabe and Drs A. Magneli and R. Collin for their kind discussions of the results at The Pennsylvania State College.

References

Danielson, G. C. (1949). *Acta Cryst.* **2**, 90.
Kay, H. F. & Vousden, P. (1949). *Phil. Mag.* (7), **40**, 1019.
Kittel, C. (1951). *Phys. Rev.* **82**, 829.
Luttinger, J. M. & Tisza, L. (1946). *Phys. Rev.* **70**, 954.
Megaw, H. D. (1946). *Proc. Phys. Soc.* **58**, 133.
Megaw, H. D. (1947). *Proc. Roy. Soc.* A, **189**, 261.
Sawaguchi, E. (1952). *J. Phys. Soc. Japan*, **7**, 110.
Sawaguchi, E., Maniwa, H. & Hoshino, S. (1951). *Phys. Rev.* **83**, 1078.
Sawaguchi, E., Shirane, G. & Takagi, Y. (1951). *J. Phys. Soc. Japan*, **6**, 333.
Shirane, G. (1952). *Phys. Rev.* **86**, 219.
Shirane, G. & Hoshino, S. (1952). *Phys. Rev.* **86**, 248.
Shirane, G., Sawaguchi, E. & Takagi, Y. (1951). *Phys. Rev.* **84**, 476.
Shirane, G. & Takeda, A. (1952). *J. Phys. Soc. Japan*, **7**, 5.
Ueda, R. & Shirane, G. (1951). *J. Phys. Soc. Japan*, **6**, 209.
Wood, E. A. (1951). *Acta Cryst.* **4**, 353.